

# Field Experiment on 5-Gbit/s Ultra-high-speed Packet Transmission Using MIMO Multiplexing in Broadband Packet Radio Access

Hidekazu Taoka  
and Kenichi Higuchi

An ultra-high-speed packet transmission experiment for achieving a transmission data rate of approximately 5 Gbit/s (spectral efficiency of 50 bit/s/Hz) was performed using a 100-MHz channel bandwidth in broadband packet radio access. The spectrum efficiency of 50 bit/s/Hz nearly approaches the upper limit in cellular environments near a cell site taking into account inter-cell interference. We describe the technology overview, experimental configuration, and field experimental results to achieve the data rate of 5 Gbit/s.

## 1. Introduction

The transmission data rate targeted by Fourth-Generation mobile communication systems called IMT-Advanced is 100 Mbit/s or greater in a cellular environment having a wide coverage area with high-mobility users and a maximum of 1 Gbit/s or greater in an indoor or hot-spot area with low-mobility users [1]. In previous field experiments applying Variable Spreading Factor (VSF)<sup>\*1</sup>-Spread Orthogonal Frequency Division Multiplexing (OFDM)<sup>\*2</sup> radio access with a channel bandwidth of 100 MHz, we achieved ultra-high-speed packet transmission with a throughput<sup>\*3</sup> of 1 Gbit/s (spectral efficiency<sup>\*4</sup> of 10 bit/s/Hz). In these experiments, we used Multiple-Input Multiple-Output (MIMO) multiplexing consisting

of 4 transmitter/receiver antennas at distances up to 300 m from the base station under mostly non-line-of-sight conditions [2]. In Europe, the Wireless world Initiative New Radio (WINNER)<sup>\*5</sup> research forum has set the target value for peak spectral efficiency in an isolated cell environment to 25 bit/s/Hz as a system requirement for next-generation mobile communications [3]. In this regard, we have also achieved an ultra-high-speed packet transmission data rate of 2.5 Gbit/s (spectral efficiency of 25 bit/s/Hz) in an actual outdoor propagation environment featuring mobile speeds of 5 to 20 km/h through the use of 6 transmitter/receiver antennas, 64-Quadrature Amplitude Modulation (QAM)<sup>\*6</sup>, and turbo coding<sup>\*7</sup> with a channel coding rate<sup>\*8</sup> of  $R = 8/9$  [4].

In packet transmission, the maximum

transmission data rate typically corresponds to peak throughput per cell. It is therefore important that we investigate the maximum achievable transmission data rate since raising the maximum transmission data rate for one user results in increasing the number of users that can be accommodated by high-speed transmission. In a completely isolated cell environment in which interference from neighboring cells is nonexistent, the maximum transmission data rate can be raised without limit by increasing the number of transmitter/receiver antennas and raising transmission power. In a multi-cell environment, however, increasing the number of transmitter/receiver antennas and raising transmission power serves to increase the amount of interference from neighboring cells. The maximum achievable trans-

\*1 **VSF**: A technique that adaptively changes the spreading factor and channel coding rate in radio transmission method that use data spreading such as W-CDMA and Spread OFDM (see \*2). VSF provides flexible support for various radio environments.

\*2 **Spread OFDM**: OFDM is a digital modulation method that converts a high-data-rate signal into multiple low-speed narrow-band signals and transmits them in parallel in the frequency domain to improve resistance to multipath interference and achieve high spectral efficiency. Spread OFDM is a radio transmission method that transmits the

same signal using multiple subcarriers and time symbols to increase received SINR (see \*9) and suppress thermal noise and inter-cell interference.

\*3 **Throughput**: The amount of data transmitted without error per unit time, i.e., the effective data transfer rate. In this article, throughput is defined as the (data rate on the transmission side)  $\times$  (number of packets received without error per unit time) / (number of packets transmitted per unit time).

\*4 **Spectral efficiency**: The number of data bits that can be transmitted per unit time per unit bandwidth.

\*5 **WINNER**: A European research forum concerned

with radio transmission technology for next-generation mobile communications. Founded in 2004.

\*6 **64QAM**: A digital modulation method in wireless communications that transmits data using 64 different phase and amplitude constellations. Be able to transmit 6 bits per symbol surpassing that of the Quadrature Phase Shift Keying (QPSK) and 16QAM.

\*7 **Turbo coding**: A type of error correction coding that achieves powerful error-correction performance through iterative decoding using reliability information in decoded results.

mission data rate is therefore determined by received Signal-to-Interference plus Noise power Ratio (SINR)<sup>\*9</sup> that takes inter-cell interference into account. We simulated a 19-cell multi-cell environment (3 sectors/cell) with a base station transmission power of 20W and distance between base stations of 500 m with the volume of traffic in neighboring cells (channel load) as a parameter. **Figure 1** shows the cumulative distribution function of received SINR obtained from this simulation. These results show that the distribution of received SINR improves as channel load becomes smaller. But it can also be seen that received SINR at nearly all locations within a cell is no more than approximately 30 dB even in the case of small channel load. We can therefore consider maximum received SINR in a cellular environment to be approximately 30 dB assuming a low channel load case. By per-

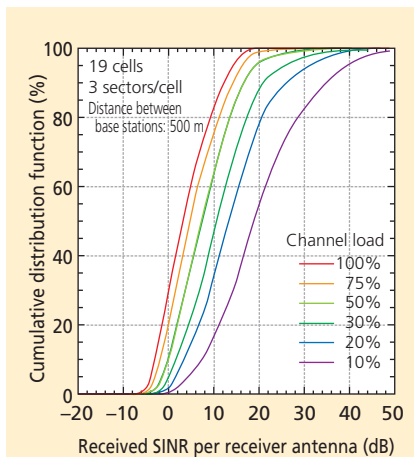


**Figure 1** Cumulative distribution function of received SINR in a cellular environment

forming computer simulations under the condition of a received SINR of 30 dB, we found that a spectral efficiency of approximately 50 bit/s/Hz could be achieved.

In this article, we describe the technology overview, experimental configuration, and results of an ultra-high-speed packet transmission field experiment using VSF-Spread OFDM<sup>\*10</sup> radio access with a 100-MHz channel bandwidth for achieving a transmission data rate of approximately 5 Gbit/s (spectral efficiency of 50 bit/s/Hz), which is practically the ultimate data rate given inter-cell interference.

## 2. Technologies for 50-bit/s/Hz Ultra-high Spectral Efficiency

We applied the following technologies for achieving ultra-high spectral efficiency of approximately 50 bit/s/Hz.

- 1) MIMO multiplexing with 12 transmitter/receiver antennas
- 2) 64QAM and turbo coding with a channel coding rate of  $R = 8/9$
- 3) Signal separation algorithm based on Maximum Likelihood Detection (MLD)<sup>\*11</sup>

The application of technologies 1) and 2) results in a transmission data rate of 4.915 Gbit/s (excluding the pilot signal and other overhead) in OFDM radio access with a channel bandwidth of 100 MHz. The application of high-accuracy signal separation technology 3) can significantly decrease required received SINR compared

to other signal separation methods.

In this signal separation method, to reduce the computational complexity of MLD that is particularly high when using higher data modulation, we applied Adaptive SElection of Surviving Symbol replica candidates (ASESS)<sup>\*12</sup> [5], a method that we previously proposed using reliability information of symbol replica candidates<sup>\*13</sup>, to complexity reduced MLD with QR decomposition<sup>\*14</sup> and M-algorithm<sup>\*15</sup> (QRM-MLD)<sup>\*16</sup> [6]. The QRM-MLD method using ASESS can greatly reduce computational complexity with almost no deterioration in throughput. This is achieved by decreasing the number of calculations of the Euclidean distance<sup>\*17</sup> required for signal separation by using reliability information for each symbol obtained simply by symbol<sup>\*18</sup> ranking using quadrant detection<sup>\*19</sup>.

When achieving a transmission data rate of 5 Gbit/s using radio transmission technologies 1) to 3) above, QRM-MLD with ASESS can reduce computational complexity to approximately  $1/(2 \times 10^{17})$  that of MLD incorporating no computation-reduction measures and to approximately 1/15 that of the original QRM-MLD method.

## 3. Structure of MIMO Multiplexing Transceivers

**Figure 2** shows the configuration of the experimental transmitter and receiver equipment that we constructed. Carrier

\*8 **Channel coding rate:** The ratio of the number of data bits to the number of bits after error correction coding (a coding rate of 8/9 means that 8 bits of data become 9 bits after performing error correction coding).

\*9 **Received SINR:** Ratio of desired received signal power to that of other received signals (interfering signals from other cells or sectors and thermal noise).

\*10 **VSF-Spread OFDM:** A radio transmission method proposed by NTT DoCoMo that applies VSF to Spread OFDM. One of the candidates for increasing system capacity in the downlink cellular environment and in hot-spot and indoor office environments for next-generation mobile communication systems.

\*11 **MLD:** A method of signal separation in MIMO multiplexing. Using the received signals of all the receiver antenna branches, this method selects the most likely combination of signal points from among all possible signal-point candidates in the

digital modulation (64QAM in this article) of each transmitter antenna branch.

\*12 **ASESS:** A method for sequentially selecting symbol replica candidates with high reliability based on the reliability information and accumulated branch metric of each symbol obtained by simple symbol ranking using quadrant detection (see \*19).

\*13 **Symbol replica candidate:** Possible signal-point candidate of each transmitter antenna branch, and received signal-point candidate calculated using estimated amount of fluctuation in channel amplitude and phase.

frequency and bandwidth are 4.635 GHz and 101.4 MHz, respectively. The transmitter (the receiver) have 12 antennas and each consist of a memory unit and radio unit, the latter including a digital-to-analog (D/A) (analog-to-digital (A/D)) converter. In this experimental system, transmitted signal generation before the D/A conversion at the transmitter and received signal demodulation after A/D conversion at the receiver are done off-line by a workstation. However, because actual RF transceivers are used for the signal transmission, the transmission performance is the same as for real-time signal transmission. **Table 1** shows the basic specifications of the Radio Frequency (RF) unit and **Table 2** the basic specifications of the baseband

signal processing unit.

In more detail, the transmitter consists of a workstation equipped with a 480-Gbyte hard disk, a memory unit with 9 Gbyte of memory per branch<sup>\*20</sup>, a 14-bit D/A converter, Intermediate Frequency (IF)<sup>\*21</sup> and RF transmission circuits, and 12 branches of transmitter antennas. First, on the workstation, after the binary information bit sequence is turbo coded (constraint length<sup>\*22</sup> = 4 bits;  $R = 8/9$ ) and bit interleaved<sup>\*23</sup>, the 64QAM data modulation mapping is performed. It then performs a serial-to-parallel conversion on the transmit symbol sequence resulting from data modulation, placing it onto 1,536 subcarriers. Next, the system time-multiplexes quadrature pilot symbols<sup>\*24</sup>

characteristic of the transmitter antennas into subframes (subframe length: 0.5 ms) and generates a symbol sequence for each transmitter antenna. The symbol sequence is converted to OFDM symbols (effective symbol length: 15.170  $\mu$ s) by a 2,048-point Inverse Fast Fourier Transform (IFFT)<sup>\*25</sup> and adds a Cyclic Prefix (CP)<sup>\*26</sup> with a duration of 2.067  $\mu$ s. The baseband modulated signal of the in-phase and quadrature components<sup>\*27</sup> after CP insertion is now stored in the memory unit of the transmitter. A D/A conversion is performed to the transmitted signals at a sampling rate of 270 Msample/s followed by quadrature modulation, conversion to a RF signal, and transmission from each antenna.

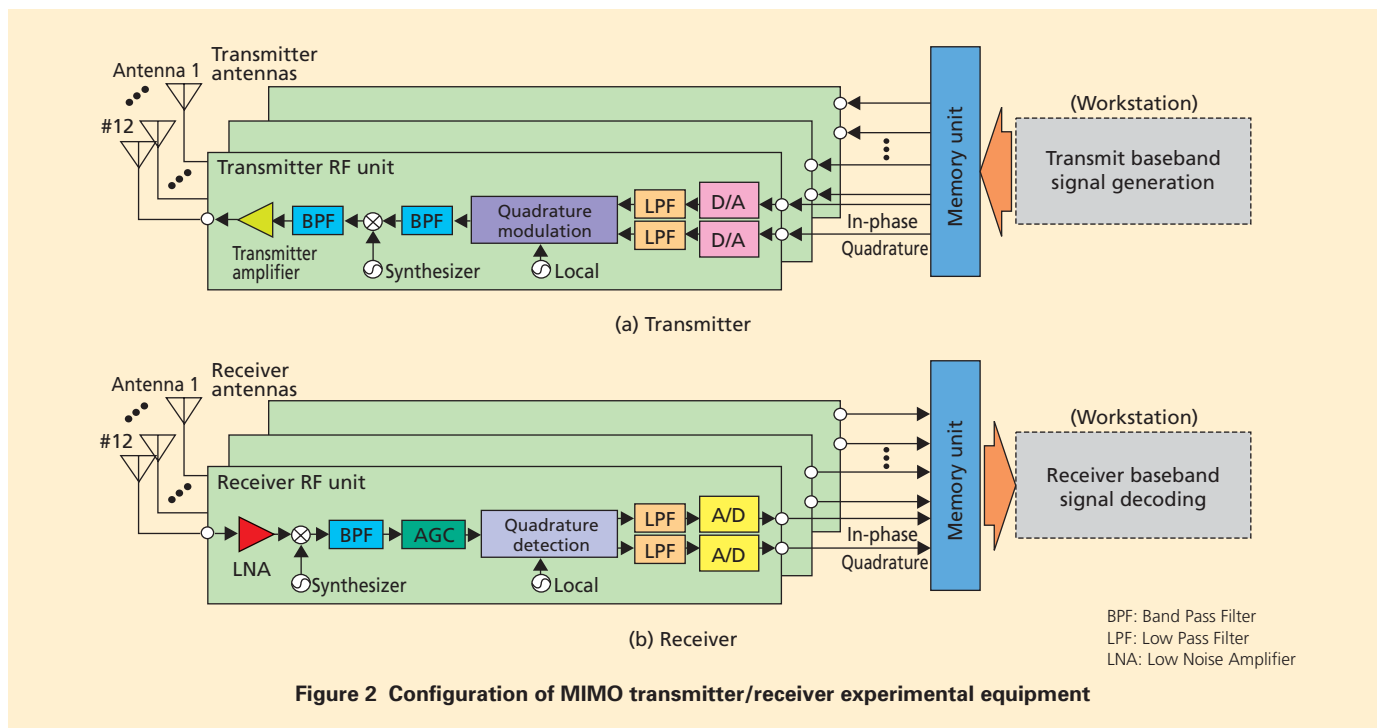


Figure 2 Configuration of MIMO transmitter/receiver experimental equipment

\*14 **QR decomposition:** A mathematical technique for decomposing any  $m$ -row  $\times n$ -column complex matrix  $H$  into the product of  $m \times n$  unitary matrix  $Q$  and  $n \times n$  upper triangular matrix  $R$  ( $H=QR$ ).  
 \*15 **M-algorithm:** A method for successively reducing symbol candidates at each stage (transmitter antenna) by selecting  $M$  ( $\leq N$ ) of  $N$  symbol replica candidates.  
 \*16 **QRM-MLD:** As in MLD, this method selects the most likely combination of signal points from among all possible signal-point candidates of each transmit antenna branch. The application of QR

decomposition and M-algorithm significantly reduces computational complexity.  
 \*17 **Euclidean distance:** The shortest distance between two points in space.  
 \*18 **Symbol:** In this article, the signal unit after error correction coding and data modulation mapping.  
 \*19 **Quadrant detection:** On the  $xy$  plane, a method for detecting which of four quadrants delimited by the  $x$  and  $y$  axes centered on the origin an entity is positioned in. Quadrant detection in this article is easily performed by simply detecting the in-phase and quadrature components of the received signal.

\*20 **Branch:** In this article, an antenna and RF transmitter or receiver.  
 \*21 **IF:** In a radio receiver circuit, specific frequencies used for improving frequency selectivity and receiver sensitivity. Although a variety of radio frequencies are used in mobile communication systems, they are commonly converted to IF before demodulation within receiver circuits.  
 \*22 **Constraint length:** Number of past input bits needed to obtain output. A longer constraint length improves error correction performance but makes for more computation in decoding.

Table 1 Basic specifications of RF unit

|   |   |
|---|---|
| Carrier frequency                             | 4.635 GHz                                 |
| Bandwidth                                     | 101.4 MHz                                 |
| No. of antennas                               | 12 (transmitter/receiver)                 |
| Base station transmission power               | 20 W (total)                              |
| No. of quantized bits in D/A (A/D) converters | 14 bit (D/A)/12 bit (A/D)                 |
| Sampling clock rate                           | 270 Msample/s                             |
| Memory (per branch)                           | 9 Gbyte (Transmitter)/18 Gbyte (Receiver) |
| Hard disk capacity                            | 480 Gbyte                                 |

Table 2 Basic specifications of baseband signal processing unit

|                          |   |
|--------------------------|---|
| Radio access             | VSF-Spread OFDM   |
| Subframe length          | 0.5 ms  |
| No. of subcarriers       | 1,536 (subcarrier separation: 65.919 kHz)               |
| OFDM symbol duration     | Data 15.170 $\mu$ s + CP 2.067 $\mu$ s                  |
| Spreading factor         | 1   |
| Channel coding/decoding  | Turbo coding ( $R=8/9$ , $K=4$ ) / Max-Log-MAP decoding |
| Window timing detection  | Pilot symbol-based window timing detection              |
| Channel estimation       | Two-dimensional MMSE channel estimation filter          |
| Signal separation method | QRM-MLD with ASESS                                      |

The receiver consists of 12 branches of receiver antennas, RF and IF receiver circuits, a 12-bit A/D converter, 18 Gbyte of memory per branch, and a workstation equipped with a 480-Gbyte hard disk. In the IF band, the received signals are linearly amplified by an Automatic Gain Control (AGC) amplifier, and then the quadrature detection and A/D conversion are performed. The baseband modulated received signal of the in-phase and quadrature components is now stored in the receiver's large-capacity memory. Next, at the workstation, the system takes this digital signal and performs Fast Fourier Transform (FFT)<sup>\*28</sup> window-timing<sup>\*29</sup> detection, and after performing CP removal, it separates the signal into each subcarrier's components. Following this, the channel estimation value<sup>\*30</sup> for each subcarrier is measured by using two-dimensional Minimum Mean Square Error (MMSE) channel estimation<sup>\*31</sup> [7], and in the signal-separation unit, signal detection is performed by QRM-MLD with ASESS using these channel estima-

tion values. Next, to perform soft-decision<sup>\*32</sup> turbo decoding, we calculate a Log Likelihood Ratio (LLR)<sup>\*33</sup> [8] for each bit from the signal output from the signal-separation unit, and after performing deinterleaving<sup>\*23</sup>, it inputs the signal into a turbo decoder (Max-Log-MAP decoding)<sup>\*34</sup> and recovers the transmit signal sequence.

## 4. Field Experimental Results

The field experiment was conducted on the measurement course shown in **Figure 3** located in the Yokosuka Research Park (YRP) district of Yokosuka City, Kanagawa prefecture, Japan. **Photo 1** shows the base station antennas and the measurement van equipped with

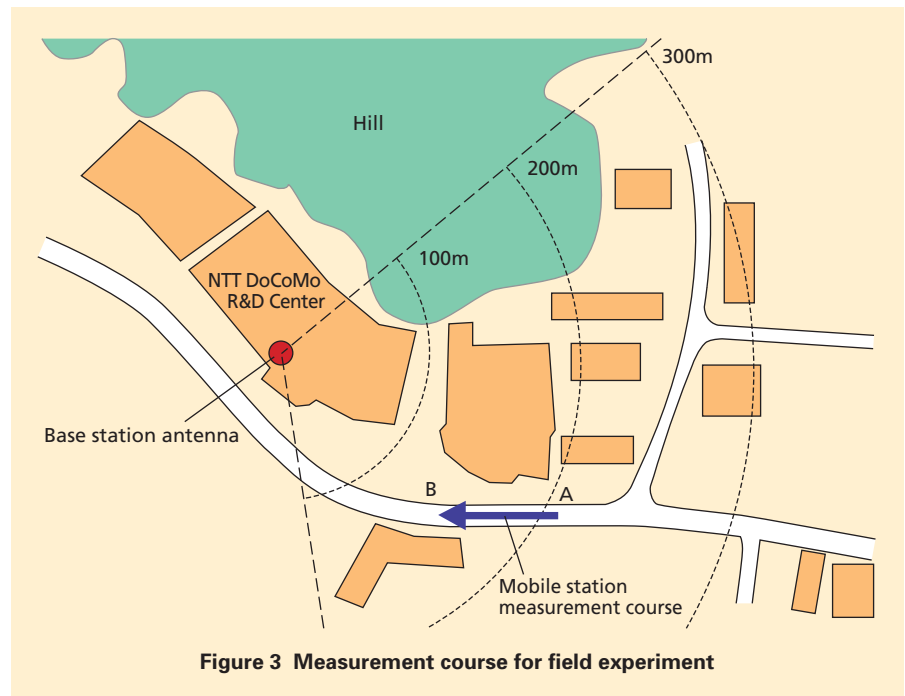


Figure 3 Measurement course for field experiment

\*23 **Interleave:** In this article, a technique for randomizing burst errors caused by fluctuation in fading in mobile communications. Combining interleaving with error correction coding raises error correction performance. Interleaving performed on a bit sequence before data modulation is called bit interleaving. Deinterleaving means returning the randomized transmit signal to its original order at the receiver.

\*24 **Pilot symbol:** A symbol that is known to both the transmitter and receiver. Used on the receiver side for symbol synchronization, for estimating

amplitude and phase fluctuation on the channel, and for estimating the received signal power, interference power, and noise power.

\*25 **IFFT:** The inverse transform of the FFT (see \*28). Generates a temporal waveform signal by the convolution of the signals of each frequency component.

\*26 **CP:** A guard interval inserted between OFDM symbols to eliminate inter-symbol interference and adjacent-subcarrier interference caused by multipath delay.

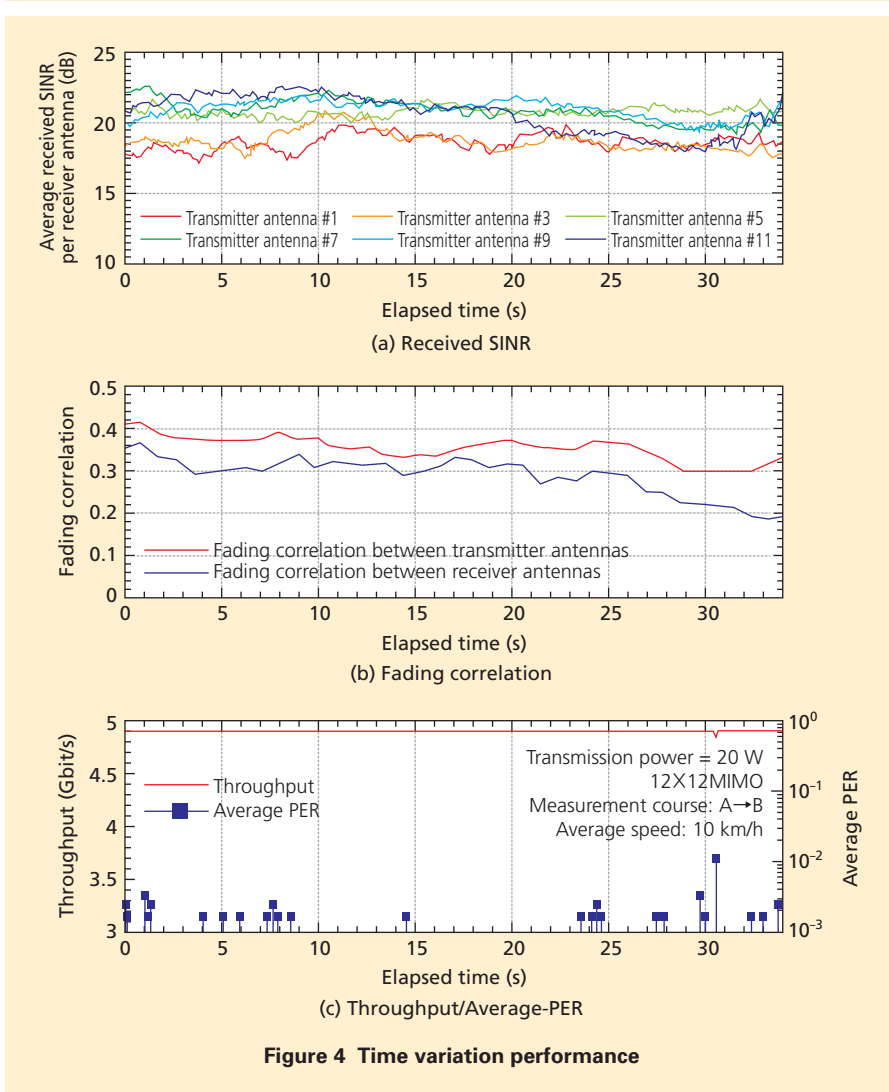
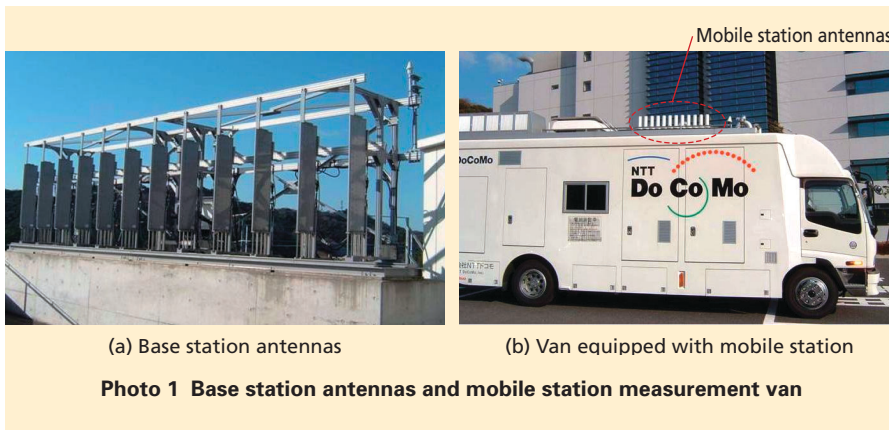
\*27 **Baseband modulated signal of the in-phase**

**and quadrature components:** In-phase and quadrature components of the digital signal before quadrature modulation (after detection).

\*28 **FFT:** A technique for quickly extracting the frequency components and their power ratios included in a signal.

\*29 **Window timing:** Receive timing for performing a FFT.

\*30 **Channel estimation value:** The estimated amount of fluctuation in the propagation path (channel) using pilot symbols time-multiplexed with data symbols within each packet frame.



mobile station antennas used in the field experiment. The transmitter antenna at the base station is a 12-branch sectored-beam antenna<sup>\*35</sup> with a 3-dB width of 90 degrees in azimuth installed at a height of approximately 26 m. The transmission power and antenna gain of each antenna were 20W and 19 dBi, respectively, and antennas are linearly arranged with an adjacent antenna separation of 70 cm (equivalent to approximately 11 wavelengths for the carrier frequency of 4.635 GHz). The mobile station used 12 dipole antennas<sup>\*36</sup> installed in a row at a height of approximately 3.5 m. The antenna gain was 2 dBi and the separation between adjacent receiver antennas was set to 20 cm (equivalent to approximately 3.1 wavelengths). In the experiment, the measurement van equipped with the mobile station was driven along the measurement course shown in Fig. 3 at an average speed of approximately 10 km/h where the distance from the transmitter was 150 to 200 m. The majority of the course is under non-line-of-sight conditions due to the surrounding office buildings that are approximately three to six stories high between the transmitter and receiver.

**Figure 4** shows the time variations in the average total received SNR per receiver antenna, the measured fading correlations between adjacent transmitter antennas, and the average Packet Error Rate (PER) along with the measured throughput using 12-by-12 MIMO multiplexing.

**\*31 Two-dimensional MMSE channel estimation:** Taking the correlation between channel fluctuation in the temporal and frequency directions into account and using pilot symbols multiplexed within fixed subcarrier intervals and time intervals, this technique performs high-accuracy estimation of frequency-and-temporal channel fluctuation in data symbols multiplexed between the pilot symbols in a way that minimizes estimation error.

**\*32 Soft-decision:** A type of decoding that adds reliability information to received symbols and uses

the value itself of the received signal based on that information. Compared to hard-decision that decodes the received signal into a binary result (0 or 1), soft-decision achieves higher error correction performance.

**\*33 LLR:** Used in soft-decision decoding. The logarithm of the ratio of reliability information (likelihood) of the required received data being 0 to the reliability information (likelihood) of the data being 1.

**\*34 Max-Log-MAP decoding:** A channel decoding algorithm. Compared to Maximum A posteriori

Probability (MAP), which is considered to be an optimal decoding algorithm, Max-Log-MAP achieves nearly equivalent characteristics while significantly decreasing computational complexity by using an approximation in the calculation of a posteriori probability.

**\*35 Sectored-beam antenna:** An antenna with directional properties used for reducing interference between adjacent sectors on a sectored base station.

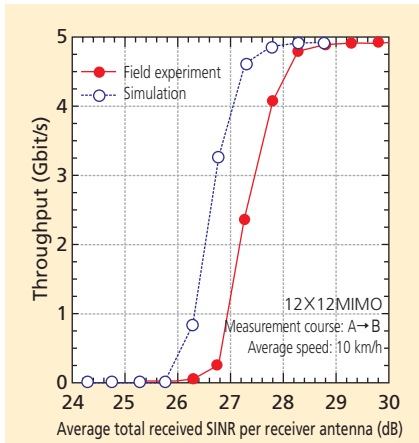


**Figure 5 Throughput performance**

Fig. 4(a) and (b) reveal that the received SINR per transmitter antenna fluctuates in the range of approximately 18 to 22 dB and that the variation in the measured fading correlation over the course is small in the range of approximately 0.2 to 0.4. Fig. 4(c) clearly shows that 4.915 Gbit/s packet transmission with an average PER below  $10^{-2}$  is achieved at most of the locations along the measurement course where the maximum distance from the base station is approximately 200 m. **Figure 5** shows the measured throughput using 12-by-12 MIMO multiplexing as a function of the average total received SINR with a receiver antenna spacing of 20 cm. The computer simulation results are also shown assuming a propagation channel condition corresponding to the average value of delay spread<sup>\*37</sup> and fading correlation between antennas along the measurement course in the field experiment. From the figure, we can see that the difference in

the required received SINR between the results of the field experiment and those of simulation is only within approximately 1 dB. This degradation is mainly due to the difference in the propagation channel model, channel estimation error, and signal detection error caused by the quantization error in the A/D converter of the implemented MIMO receiver. Fig. 5 also shows that the peak throughput of 4.915 Gbit/s, i.e., the frequency efficiency of approximately 50 bit/s/Hz, is achieved at an average total received SINR per receiver antenna of approximately 28.5 dB when the receiver antenna spacing is 20 cm by adopting the QRM-MLD signal detection method with ASESS.

## 5. Conclusion

We described the technology behind an ultra-high-speed packet transmission field experiment using VSF-Spread OFDM radio access for achieving a maximum transmission data rate of approximately 5 Gbit/s with a 100-MHz channel bandwidth and presented field experimental results. Using MIMO multiplexing consisting of 12 transmitter/receiver antennas in an actual outdoor propagation environment, we showed that ultra-high-speed packet transmission with a maximum throughput of approximately 5 Gbit/s (spectral efficiency of approximately 50 bit/s/Hz) could be achieved with a required average total received SINR of approximately 28.5 dB.

## REFERENCES

- [1] ITU-R Recommendation M.1645.
- [2] H. Taoka, K. Higuchi and M. Sawahashi: "Field Experiments on Real-Time 1-Gbps High-Speed Packet Transmission in MIMO-OFDM Broadband Packet Radio Access," in Proc. IEEE VTC2006-Spring, Vol. 4, pp. 1812-1816, May 2006.
- [3] IST-2003-507581, D7.1 v1.0, System Requirements, WINNER, Jul. 2004.
- [4] H. Taoka, K. Dai, K. Higuchi and M. Sawahashi: "Field experiments on 2.5-Gbps packet transmission using MLD-based signal detection in MIMO-OFDM broadband packet radio access," in Proc. WPMC2006, Sep. 2006.
- [5] K. Higuchi, H. Kawai, N. Maeda and M. Sawahashi: "Adaptive Selection of Surviving Symbol Replica Candidates Based on Maximum Reliability in QRM-MLD for OFCDM MIMO Multiplexing," in Proc. IEEE Globecom 2004, pp. 2480-2486, Nov. 2004.
- [6] K. J. Kim and J. Yue: "Joint channel estimation and data detection algorithms for MIMO-OFDM systems," in Proc. Thirty-Sixth Asilomar Conference on Signals, Systems and Computers, pp. 1857-1861, Nov. 2002.
- [7] O. Edfors, M. Sandell, J.-J. Beek, S. Kate and P. O. Borjesson: "OFDM channel estimation by singular value decomposition," IEEE Trans. Commun., Vol. 46, No.7, pp. 931-939, Jul. 1998.
- [8] K. Higuchi, H. Kawai, N. Maeda, M. Sawahashi, T. Itoh, Y. Kakura, A. Ushirokawa and H. Seki: "Likelihood function for QRM-MLD suitable for soft-decision turbo decoding and its performance for OFCDM MIMO multiplexing in multipath fading channel," in Proc. IEEE PIMRC 2004, pp. 1142-1148, Sep. 2004.

\*36 **Dipole antenna:** The simplest of all antennas, comprising two straight, linearly-aligned conductor wires (elements) attached to the end of a cable (feed point).

\*37 **Delay spread:** For radio propagation in mobile communications, the spread in delay time of all paths (waves) arriving late because of reflection or diffraction from buildings or other objects. Defined by a standard deviation determined by weighted statistical processing on delaytime of all

arriving paths (waves), using received signal power.

***Hidekazu Taoka***

**Assistant Manager,  
Radio Access Network Development Department**

Joined in 2000. Engaged in the R&D of wireless access technology for Fourth-Generation mobile communication systems. A member of IEICE.

***Kenichi Higuchi***

**Assistant Manager,  
Radio Access Network Development Department**

Joined in 1994. Engaged in the R&D of wireless access technology for W-CDMA/Fourth-Generation mobile communication systems. Serving as both a lecturer in the Faculty of Science and Technology at the Tokyo University of Science and as Assistant Manager in the Radio Access Network Development Department since 2007. Ph. D., Engineering. A member of IEICE and IEEE.